Accepted Manuscript

Novel deoxyvasicinone derivatives as potent multitarget-directed ligands for the treatment of Alzheimer's disease: Design, synthesis, and biological evaluation

Fang Ma, Hongtao Du

PII: S0223-5234(17)30690-6

DOI: 10.1016/j.ejmech.2017.09.008

Reference: EJMECH 9723

To appear in: *European Journal of Medicinal Chemistry*

Received Date: 11 July 2017

Revised Date: 3 September 2017

Accepted Date: 5 September 2017

Please cite this article as: F. Ma, H. Du, Novel deoxyvasicinone derivatives as potent multitarget-directed ligands for the treatment of Alzheimer's disease: Design, synthesis, and biological evaluation, *European Journal of Medicinal Chemistry* (2017), doi: 10.1016/j.ejmech.2017.09.008.

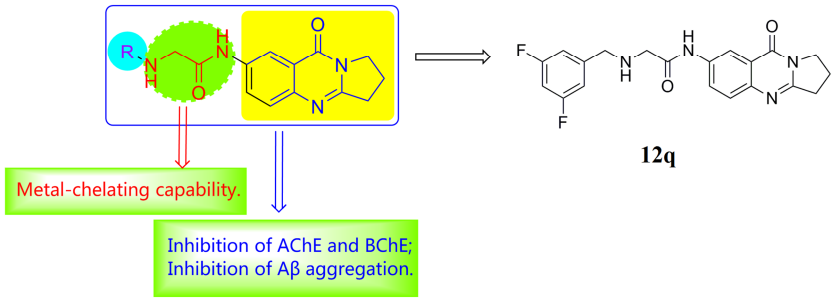

IC_{50} (*h*AChE) = 7.61 nM

IC_{50} (*h*BChE) = 2.35 nM

Aβ_{1-42} aggregation: 63.9 % at 10 μM

Chelation of the metal ions

Novel Deoxyvasicinone Derivatives as Potent Multitarget-Directed Ligands for the Treatment of Alzheimer's Disease: Design, Synthesis, and Biological Evaluation

Fang Ma [b] , Hongtao Du [a, c, *]

[a] College of Life Sciences, Xinyang Normal University, Xinyang, Henan, China

[b] School of Geographic Sciences, Xinyang Normal University, Xinyang, Henan, China

[c] Shaanxi Key Laboratory of Natural Products & Chemical Biology，School of Chemistry and Pharmacy, Northwest A&F University, Yangling 712100, Shaanxi Province, P. R. China.

E-mails: duht@nwsuaf.edu.cn (H. T. Du); mafang_1984@163.com (F.Ma)

***Corresponding author:**

Dr. Hong-Tao Du

1. College of Life Sciences, Xinyang Normal University, Xinyang, Henan 464000, P. R. China

2. Shaanxi Key Laboratory of Natural Products & Chemical Biology, College of Sciences, Northwest A&F University, Yangling, Shaanxi 712100, P. R. China

Email: duhongtao8410@163.com

ABSTRACT

A series of multitarget ligands was designed by introducing several structurally diverse aminoacetamide groups at position 6 of the deoxyvasicinone group, with the aim of obtaining novel multifunctional anti-Alzheimer's disease agents using deoxyvasicinone as the substrate. *In vitro* studies showed that almost all of the derivatives were potent inhibitors of human recombinant acetylcholinesterase (*h*AChE) and human serum butyrylcholinesterase (*h*BChE), with IC_{50} values in the low nanomolar range, and exhibited moderate to high inhibition of Aβ_{1-42} self-aggregation. In particular, compounds **12h**, **12n**, and **12q** showed promising inhibitory activity for *h*AChE, with IC_{50} values of 5.31 ± 2.8, 4.09 ± 0.23, and 7.61 ± 0.53 nM, respectively. Compounds **12h** and **12q** also exhibited the greatest ability to inhibit *h*BChE, with IC_{50} values of 4.35 ± 0.32 and 2.35 ± 0.14 nM, respectively. Moreover, enzyme kinetics confirmed that compound **12q** caused a mixed type of AChE inhibition, by binding to both the active sites (PAS and CAS) of AChE. Remarkably, compound **12q** also demonstrated the highest potential inhibitory activity for Aβ_{1-42} self-aggregation (63.9 ± 4.9%, 10 μM), and it was also an excellent metal chelator.

KEYWORDS

Alzheimer's disease; deoxyvasicinone derivatives; cholinesterase inhibitors; inhibition of Aβ_{1-42} self-aggregation; metal chelator

1. Introduction

Alzheimer's disease (AD) is a progressive and degenerative neurodegenerative brain disorder characterized by loss of neurons and synapses in the cerebral cortex and certain subcortical regions[1]. AD is the most common form of dementia, affecting approximately 47 million people worldwide in 2015[2]. With the increase in average life expectancy, the number of affected persons is projected to exceed 100 million individuals worldwide by 2050[3]. Clinically, the symptoms can include problems such as loss of memory, language deterioration, mood swings, and loss of bodily functions, ultimately leading to death[4]. At this time, acetylcholinesterase (AChE) inhibitors (tacrine (**1**), donepezil (**2**), rivastigmine (**3**), and galantamine (**4**), Figure 1) and *N*-methyl-D-aspartate antagonist are the only approved drugs that can provide a palliative, therapeutic strategy in mild forms of AD[5, 6]. Unfortunately, there is no means to cure, or even slow, the progression of the disease[7]. This alarming situation needs further effort to develop more effective drugs for treatment of AD.

Although the exact cause of AD is still not fully known, the consensus is that AD is a multifactorial disease[8]. Low levels of acetylcholine (ACh) in the hippocampus and cortex area of the brain, deposition of amyloid-β (Aβ) peptide, neurofibrillary tangles (*p*-Tau), and oxidative stress are thought to play vital roles in AD pathogenesis[9-12]. Because of the complexity of AD and the interconnection of molecular events in its progression, the single-target directed drugs that have reached clinical trials have failed. Therefore, some researchers have invested their efforts in the design of multitarget-directed ligands (MTDLs) [13-15], which simultaneously interact with two or more diseased targets, as a better strategy for AD rather than concentrating on reducing just one target.

Aβ plays an important role among the multiple factors in AD[16]. Neurofibrillary tangles and aggregated Aβ peptide deposition in senile plaques have been identified as the main pathological hallmarks[17-19]. Thus, drugs that are expected to reduce Aβ production, prevent Aβ aggregation, and promote Aβ clearance are promising approaches for the treatment of AD[20].

AD is ascribed to reduced levels of ACh, which is an important neurotransmitter involved in memory and learning in the brain[21]. AChE inhibitors (AChEIs) can increase the amount of ACh in the synaptic cleft. Recent studies have also shown that AChEIs possibly affect the expression and/or the metabolic processing of amyloid precursor protein, which may influence Aβ generation[22, 23]. Therefore AChEIs remain the preferred target for the treatment of AD[24, 25]. Recently, some articles have reported that butyrylcholinesterase (BChE), another cholinesterase present in the brain, has the similar biological function as AChE for hydrolysis of ACh in a healthy human brain[26]. Moreover, BChE inhibitors (BChEIs) not only improve the cognitive performance of aged rats without the classic adverse effects associated with AChE inhibition but they also inhibit amyloid fibril formation[27]. Furthermore, inhibitors of both of these cholinesterase enzymes have shown significant clinical utility in conferring cognitive improvements. Thus, developing MTDLs with dual inhibitors may have benefits for the treatment of AD[28, 29].

Biometals, including Cu(II), Zn(II), and Fe(II, III), have also been found to promote aggregation of Aβ[30, 31]. In addition, the interaction of Aβ with Cu(II) is involved in the production of reactive oxygen species and oxidative stress[32], which implies that modulation of these biometals in the brain may be a potential therapeutic strategy for the treatment of AD[33, 34].

Deoxyvasicinone (**5**) (Figure 2), consisting of a quinazolinone moiety conjugated with a pyrrolidine, is a naturally occurring alkaloid with antibacterial[35], antiinflammatory[36], and

antiproliferative activities[37]. Structure−activity relationships (SARs) of the quinazolinone ring system examined in various studies suggest that position 6 is suitable for substituents[38-41]. Recently, deoxyvasicinone and its derivatives have been considered as cholinesterase inhibitors, because the structure of deoxyvasicinone is similar to that of tacrine (**1**). Deoxyvasicinone exhibits moderate inhibitory activity towards AChE (from Electric Eel) and BChE (from equine serum), with IC_{50} values of 82.5 and 25.1 μM, respectively[39]. Compounds **6** and **7** demonstrate dramatic inhibitory activities towards AChE and BChE, with IC_{50} values of 69.2 nM and 1.95 μM, respectively[40, 41]. In addition, there are several reports that suggest that carbamate-containing compounds (e.g., rivastigmine (**3**) and compounds **7** and **8**) can be used for BChE-inhibiting activity[41,42]. We assume that the effects of the aminoacetamide structure on BChE-inhibitory activity is similar to that of carbamate. Furthermore, the aminoacetamide structure also has metal ion complexing action. On the basis of the forgoing, we introduced different aminoacetamide groups into the 6 position of deoxyvasicinone, to obtain a novel series of derivatives that are expected to be AChEIs and BChEIs, inhibitors of self-induced A*β* aggregation, and biometal chelators. For investigation into the SARs of this class of compounds, several hydrophobic substituents (aliphatic and aromatic moieties) were added to the aminoacetamide groups (Figure 3).

2. Results and discussion

2.1. Chemistry

The synthetic route to compounds **12a−12s** is depicted in Scheme 1. The starting material deoxyvasicinone (**5**) was synthesized as previously described[35]. A nitration reaction of compound deoxyvasicinone with H_2SO_4−HNO_3 provided the nitration product, which was reduced by

$Na_2S \cdot 9H_2O$ in the presence of sodium hydroxide as a base, to afford compound **10.** The nucleophilic substitution reaction of compound **10** with different bromohydrocarbons using sodium hydride as a base with a catalytic amount of potassium iodide in acetonitrile as a solvent yielded the target compounds **11a−11s**. Finally, compounds **12a−12s** were obtained after the deprotection of the Boc group in the presence of CF_3COOH and dry dichloromethane.

2.2. In Vitro AChE and BChE Inhibition Assays

The inhibitory activities of the synthesized compounds **12a−12s** against human recombinant AChE (*h*AChE) and human serum BChE (*h*BChE) were evaluated by the method of Ellman et al., where tacrine (**1**) and deoxyvasicinone (**5**) were used as reference compounds. IC_{50} values and selectivity ratios are listed in Table 1.

It is evident that the synthesized derivatives were potent inhibitors of *h*AChE, with IC_{50} values in the low nanomolar range. Furthermore, all compounds showed much stronger inhibitory activity than the parent compound (deoxyvasicinone (**5**), IC_{50} = 62.5 μM). Encouragingly, 14 of the 19 derivatives displayed higher inhibitory activity against *h*AChE than that of the positive control (tacrine (**1**), IC_{50} = 76.5 nM). Notably, compounds **12h**, **12n**, and **12q** exhibited very potent AChE inhibitory activity, with IC_{50} values of 5.31, 4.09, and 7.61 nM, respectively. In addition, several SARs were observed. The inhibitory potency of these derivatives (except for compounds **12f** and **12g**) against *h*AChE was enhanced with increasing length of the carbon chain (**12a** vs. **12b** vs. **12c** vs. **12d** vs. **12e** vs. **12h**, **12i** vs. **12j**, and **12m** vs. **12n**). These findings are in accordance with the results from Decker's group[40]. On lengthening the tether chain from 2 to 16 carbon units, the inhibitory activity against *h*AChE increased by between 112-fold and 11,770-fold (**12a** vs. **12h**). The inhibitory activity also

increased with the degree of unsaturation: for example, compounds **12i** and **12l**, with an unsaturated group, exhibited higher AChE inhibitory activity (IC_{50} = 66.6 and 46.4 nM, respectively) than the derivative with a saturated group (**12b**, IC_{50} = 557 nM). When aromatic groups were added to the aminoacetamide moiety, *h*AChE inhibitory activity increased in the presence of electron-donating substituents in the *o*-position or when the conjugated system was enlarged (**12m** vs. **12o** vs. **12p** vs. **12r** vs. **12s**). These results imply that extending the conjugated system could improve the combination of derivatives and *h*AChE.

It is of note that, in MTDLs, strong AChE inhibitory activity is just one part of the rationale behind the development of such synthetic molecules. Evidence suggests that BChE is primarily expressed and secreted by glial cells, and its level remains constant or increases in advanced AD, while AChE concentration in certain brain regions decreases[27]. Inhibition of central BChE activity has also been researched as a potential therapeutic approach to ameliorate the cholinergic deficit in moderate forms of AD[29,43]. These reports show that balanced inhibition of both cholinesterases could be conducive to the treatment of AD[28]. Thus, the test compounds were also evaluated for *h*BChE inhibitory activity, and the results are summarized in Table 1.

As planned in the compound design, the synthesized compounds exhibited potent *h*BChE inhibitory activity (IC_{50} values ranging from 1.186 μM to 2.35 nM), much higher than that of the parent compound (deoxyvasicinone (**5**), IC_{50} = 45.1 μM). Two derivative compounds (**12h** and **12q**) displayed better inhibitory activity against *h*BChE (IC_{50} value of 4.35 and 2.35 nM, respectively) than the positive control (tacrine (**1**), IC_{50} = 10.8 nM). Remarkably, compounds **12h** and **12q** also showed potent *h*AChE inhibitory activity (IC_{50} = 5.31 and 7.61 nM, respectively). These results indicate that the two candidate drugs could be effective in treating mild to moderate as well as severe

forms of AD when AChE takes over the role played by BChE. In addition, when a saturated alkyl or an aromatic group was incorporated in the aminoacetamide moiety, the SARs toward *h*BChE revealed similar trends to those observed for *h*AChE. However, with an unsaturated alkyl in the aminoacetamide group, a slightly different trend was observed: for example, compound **12i**, which has an allyl group, showed higher inhibitory activity against *h*BChE (IC_{50} = 16.6 nM) than the derivative with a but-1-en-4-yl group (**12j**, IC_{50} = 81.5 nM). These results show that deoxyvasicinone derivatives featuring aminoacetamide groups exhibit higher inhibitory activity against *h*AChE and *h*BChE than compounds with carbamate groups.

2.3. Kinetic Evaluation of Compound 12q on hAChE

To assess the AChE inhibition mechanism of deoxyvasicinone derivatives, the potent compound **12q** was chosen for an enzyme kinetic study. Lineweaver−Burk reciprocal plots were constructed by plotting the double reciprocal of the increasing inhibitor and substrate concentrations (Figure 4). The plots reveal both increasing slopes (decreased V_{max}) and intercepts (higher K_m) at increasing concentrations of compound **12q**. This pattern indicated a mixed-type inhibition. The results suggest that compound **12q** could bind simultaneously to the catalytic active site (CAS) as well as to the peripheral anionic site (PAS) of *h*AChE. This is a desirable effect for treatment of AD because Aβ aggregation is catalyzed by the PAS of AChE. The inhibitor dissociation constants K_i for the enzyme−inhibitor and K'_i for the enzyme−substrate−inhibitor were estimated to be 9.85 and 15.81 nM, respectively (Supporting Information, Table S1 and Figure S1).

2.4. Inhibition of Aβ1−42 Self-aggregation Assay

Aβ_{1-42} aggregation is deemed to play a crucial role in the pathogenesis of AD[44]. Thus, the inhibition of Aβ_{1-42} self-aggregation has been investigated as an attractive therapeutic strategy to more efficiently combat AD[45]. In this work, inhibitory activity of the deoxyvasicinone derivatives against Aβ_{1-42} self-aggregation was evaluated using the thioflavin T fluorescence assay[46], with deoxyvasicinone and curcumin as reference compounds. The results (Table 1) show that the derivatives exhibited moderate to good potencies, with inhibition in the range 6.46−63.9% at 10 μM. It is interesting that most of substituted alkyl groups in the aminoacetamide moiety generally enhanced inhibition activity with increasing length of the carbon chain (with the exception of compound **16**). Compounds **12m−12s**, with a substituted benzyl group in the aminoacetamide moiety, generally gave better results for inhibition activity (25.0−63.9%): compound **12q**, with a 3,5-difluorobenzyl group in the aminoacetamide moiety, was the most potent inhibitor of Aβ_{1-42} aggregation (63.9%). Compound **12b**, with a propyl group in the aminoacetamide moiety, exhibited inhibition activity of 7.38%. On the other hand, compounds **12i** and **12l**, with an allyl and propargyl group in the aminoacetamide moiety, respectively, led to 37.9% and 52.3% inhibition, respectively. These results imply that increased unsaturation of substituents in the aminoacetamide group could improve inhibitory activity.

2.5. Metal-Chelating Properties of Compound 12q

The ability of compound **12q** to bind biometals such as Cu(II), Fe(II), Fe(III), and Zn(II) was investigated by ultraviolet–visible (UV−vis) and fluorescence spectrometry[47, 48], and the results are shown in Figure 5. Cu(II), Fe(II), and Fe(III) cause an impressive decrease in the intrinsic

fluorescence of compound **12q** (Figure 5A), and this effect increases in a dose-dependent manner with concentration. However, the fluorescence intensity of compound **12q** did not differ substantially in the absence or presence of Zn(II) (Supporting Information, Figure S2). In addition, after $CuSO_4$ was added to a solution of compound **12q**, the maximum absorption wavelength shifted from 282 to 291 nm, indicating the formation of a **12q**−Cu(II) complex (Figure 5B). The maximum absorption at 282 nm decreased with the addition of $FeSO_4$ and $FeCl_3$, which suggests that Fe(II) and Fe(III) possibly interacted with compound **12q.** However, when $ZnCl_2$ was added, there was no significant change in the UV spectrum, which is in accordance with the fluorescence spectrum.

To determine the binding stoichiometry of compound **12q** with Cu(II), the UV spectra were used to measure the absorbance of the complex of compound **12q** and Cu(II) at different concentrations at 451 nm. As depicted in Figure 5C, when the absorbance changes at 451 nm were plotted, two straight lines intersected at a mole fraction of 0.86, indicating a 1:1 stoichiometry for the complex **12q**−Cu(II).

3. Conclusion

In summary, all 19 deoxyvasicinone derivatives exhibited high *h*AChE and *h*BChE inhibitory activity at nanomolar concentrations. In particular, inhibitory activities against *h*AChE (IC_{50} = 7.61 nM) and *h*BChE (IC_{50} = 2.35 nM) of one derivative (**12q**) increased 8729- and 19191-fold in comparison with the parent compound. Remarkably, compound **12q** also demonstrated the highest potential inhibitory activity for $A\beta_{1-42}$ self-aggregation (63.9 ± 4.9%, 10 μM), and it was also an excellent metal chelator. Thus, compound **12q** is a promising multifunctional candidate for the treatment of AD. Further investigations of AD therapeutic candidates are in progress, and results will

be presented later. Meanwhile these beneficial effects of the derivatives highlight deoxyvasicinone as a lead molecule and aminoacetamide structure as a rewarding group to be developed in the search for multi-target drugs for the treatment of AD.

4. Experimental part

4.1. General Remarks.

All reagents were commercial grade, and were used without further purification unless otherwise indicated. Silica gel (100–200 mesh) for column chromatography and silica GF_{254} for thin-layer chromatography were obtained from the Qingdao Marine Chemical Company (China). Melting points were measured using an XT-4 melting-point apparatus, and were uncorrected. ^{1}H nuclear magnetic resonance (NMR) (500 MHz) and ^{13}C NMR (125 MHz) spectra were recorded on a Bruker Avance using $CDCl_3$ or deuterated dimethyl sulfoxide (DMSO-d_6) as the solvent and tetramethylsilane as the internal standard. Chemical shifts are reported in parts per million (ppm). Multiplicities are reported as follows: singlet (s), doublet (d), triplet (t), doublet of doublet (dd), doublet of doublet of doublet (ddd) and multiplet (m). Electron ionization mass spectroscopy (ESI-MS) was undertaken with a Thermo Fisher spectrometry instrument.

4.2. Chemistry

4.2.1. Synthesis of deoxyvasicinone (5)

The deoxyvasicinone (**5**) was synthesized according to a previously described method (Supporting Information,Scheme S1)[35]. White solid, yield: 54 %. Mp: 108−109 °C. ^{1}H NMR (500 MHz, $CDCl_3$) δ 8.29 (dd, J = 8.5, 1.3 Hz, 1H), 7.73 (ddd, J = 8.5, 7.6, 1.5 Hz, 1H), 7.65 (d, J = 7.8

Hz, 1H), 7.49–7.41 (m, 1H), 4.22 (t, *J* =7.3 Hz 2H), 3.19 (t, *J* = 8.0 Hz, 2H), 2.35–2.24 (m, 2H). ^{13}C NMR (126 MHz, $CDCl_3$) δ 170.6, 169.0, 158.7, 143.7, 136.4, 136.0, 135.8, 130.1, 56.1, 42.1, 29.1. ESIMS calcd for $C_{11}H_{10}N_2O$ $[M+H]^+$,187.09; Found, 187.13.

4.2.2. Synthesis of compounds 9 and 10

A cold solution (25 mL, −10 °C) of H_2SO_4−HNO_3 (2:3, *v*/*v*) was added 0.931 g (5 mmol) of deoxyvasicinone (**5**) with stirring, and the reaction mixture was kept at −10 °C for 3 h. Upon completion of the reaction, the solution was poured into ice water, basified with 20% aq. NaOH at pH 9, and extracted with ethyl acetate. The combined extracts were washed with water, brine, dried over anhydrous Na_2SO_4. Evaporation of the solvent under reduced pressure gave a nitration product. Afterwards, a solution of nitration product in EtOH (50 mL) was added slowly to a suspension of sodium sulfide hydrate (2.420 g, 10 mmol) and NaOH (0.802 g, 20 mmol) in distilled water (80 mL). The mixture was heated to reflux for 4 h. After cooling, the solution was concentrated under reduced pressure. The compound **9** (0.792 g, 79 % yield) was isolated as a yellow solid by a column chromatography on elution with CH_2Cl_2/MeOH (10:1, *v*/*v*)

A suspension of the compound **9** (0.509 g, 2.5 mmol) in dichloromethane (30 mL) was added slowly to a solution of 1-ethyl-3-(3-dimethylaminopropyl)carbodiimide hydrochloride (0.566g, 3 mmol) and 2-((tert-butoxycarbonyl)amino)acetic acid (0.524 g, 3 mmol) in dichloromethane (40 mL). The mixture was refluxed for 6 h and concentrated in vacuum. The reaction solution was washed with water, brine, dried over anhydrous Na_2SO_4, and concentrated in vacuum to give the crude product (**10)** as a yellow solid.

4.2.3. General procedure for the preparation of compounds 11a−11s and 12a−12s

A mixture of compound **10** (127 mg, 0.5 mmol), KI (17 mg, 0.1 mmol), NaH (18 mg, 0.75 mmol),

and the alkyl bromide (1 mmol) in acetonitrile (50 mL) was refluxed. When the compound **10** disappeared (as detected by TLC), the solvents were removed under reduced pressure. Distilled water (50 mL) was then added, and the mixture was extracted with ethyl acetate (50 mL × 3). The organic solvent phase was washed by water (15 mL × 2), brine (15 mL × 2), dried over anhydrous Na_2SO_4, and evaporated under vacuum. The compounds **11a−11s** were purified by a flash chromatography on silica gel. CF_3COOH (1 mL, 14 mmol) was then added dropwise to a solution of compound **11a−11s** in dry CH_2Cl_2 (50 mL). The solution was refluxed for 7 h. After cooling, the solvent was concentrated under reduced pressure to give a yellow oil, which was purified by a flash chromatography on silica gel using CH_2Cl_2/MeOH as the elution system to obtain the compound ***12a−12s***.

2-(ethylamino)-N-(9-oxo-1,2,3,9-tetrahydropyrrolo[2,1-b]quinazolin-7-yl)acetamide ***(12a)***. White solid, yield: 53 %. Mp: 198−199 °C. ^{1}H NMR (500 MHz, DMSO-d_6) δ 9.80 (s, 1H), 8.41 (d, J = 2.5 Hz, 1H), 7.97 (dd, J = 8.8, 2.5 Hz, 1H), 7.52 (d, J = 8.1, 1H), 4.22 (s, 1H), 4.10 (t, J =7.3 Hz, 2H), 3.17 (s, 2H), 3.10 (t, J = 7.9 Hz, 2H), 2.66 (m, 2H), 2.26−2.21 (m, 2H), 1.13 (t, J = 6.2 Hz, 3H). ^{13}C NMR (126 MHz, $CDCl_3$) δ 172.3, 166.4, 160.3, 145.6, 136.5, 126.9, 126.2, 120.8, 115.2, 57.9, 48.6, 47.6, 32.3, 19.5, 13.1. ESIMS calcd for $C_{15}H_{18}N_4O_2$ $[M+H]^+$,286.33; Found, 286.34.

N-(9-oxo-1,2,3,9-tetrahydropyrrolo[2,1-b]quinazolin-7-yl)-2-(propylamino)acetamide ***(12b)***. White solid, yield: 53 %. Mp: 292−294 °C. ^{1}H NMR (500 MHz, DMSO-d_6) δ 10.15 (s, 1H), 8.44 (d, J = 2.5 Hz, 1H), 7.95 (dd, J = 8.8, 2.5 Hz, 1H), 7.56 (dd, J = 8.6, 1H), 4.25 (s, 1H), 4.10 (t, J =7.3 Hz, 2H), 3.20 (s, 2H), 3.13 (t, J = 7.9 Hz, 2H), 2.69 (t, J = 7.1 Hz, 2H), 2.29−2.24 (m, 2H), 1.40−1.32 (m, 2H), 0.96 (t, J = 6.8 Hz, 3H). ^{13}C NMR (126 MHz, $CDCl_3$) δ 166.9, 164.4, 161.2, 143.2, 137.7, 135.0, 129.5, 122.5, 114.8, 55.8, 55.0, 43.9, 33.5, 29.1, 23.2, 14.3. ESIMS calcd for $C_{16}H_{20}N_4O_2$

[M+H]$^+$, 301.36; Found, 301.36.

2-(butylamino)-N-(9-oxo-1,2,3,9-tetrahydropyrrolo[2,1-b]quinazolin-7-yl)acetamide ***(12c)***. White solid, yield: 58 %. Mp: 157−158 °C. ^{1}H NMR (500 MHz, DMSO-d_6) δ 10.49 (s, 1H), 8.46 (d, J = 2.4 Hz, 1H), 7.95 (dd, J = 8.8, 2.5 Hz, 1H), 7.56 (d, J = 8.8 Hz, 1H), 4.21−3.96 (m, 3H), 3.27 (s, 2H), 3.09 (t, J = 7.9 Hz, 2H), 2.71 (t, J = 7.1 Hz, 2H), 2.29−2.24 (m, 2H), 1.43−1.30 (m, 4H), 0.88 (t, J = 6.8 Hz, 3H). ^{13}C NMR (126 MHz, $CDCl_3$) δ 166.5, 162.5, 159.6, 147.3, 139.5, 127.8, 127.0, 122.9, 114.9, 53.6, 52.9, 46.8, 36.4, 29.5, 25.4, 19.5, 15.6. ESIMS calcd for $C_{17}H_{22}N_4O_2$ [M+H]$^+$, 315.18; Found, 315.20.

2-(hexylamino)-N-(9-oxo-1,2,3,9-tetrahydropyrrolo[2,1-b]quinazolin-7-yl)acetamide ***(12d)***. White solid, yield: 44 %. Mp: 211−213 °C. ^{1}H NMR (500 MHz, DMSO-d_6) δ 10.47 (s, 1H), 8.46 (d, J = 2.4 Hz, 1H), 7.93 (dd, J = 8.8, 2.5 Hz, 1H), 7.61 (d, J = 8.8 Hz, 1H), 4.21−3.96 (m, 3H), 3.12 (s, 2H), 3.11 (t, J = 7.9 Hz, 2H), 2.53 (t, J = 7.1 Hz, 2H), 2.26−2.21 (m, 2H), 1.38 (m, 2H), 1.29−1.28 (m, 6H), 0.81 (t, J = 6.8 Hz, 3H). ^{13}C NMR (126 MHz, $CDCl_3$) δ 166.5, 160.3, 159.6, 145.6, 136.9, 127.0, 126.2, 120.9, 114.9, 53.1, 52.5, 46.8, 32.2, 29.5, 28.9, 28.2, 27.6, 19.5, 12.3. ESIMS calcd for $C_{19}H_{26}N_4O_2$ [M+H]$^+$, 343.21; Found, 315.24.

*2-(octylamino)-N-(9-oxo-1,2,3,9-tetrahydropyrrolo[2,1-b]quinazolin-7-yl)acetamide(**12e**).* White solid, yield: 47 %. Mp: 145−146 °C. ^{1}H NMR (500 MHz, DMSO-d_6) δ 10.07 (s, 1H), 8.46 (d, J = 2.4 Hz, 1H), 7.93 (dd, J = 8.8, 2.5 Hz, 1H), 7.61 (d, J = 8.8 Hz, 1H), 4.21−3.82 (m, 3H), 3.13 (s, 2H), 3.10 (t, J = 7.9 Hz, 2H), 2.53 (t, J = 7.1 Hz, 2H), 2.23−2.18 (m, 2H), 1.38 (m, 2H), 1.29 (m, 2H), 1.28−1.26 (m, 8H), 0.80 (t, J = 6.8 Hz, 3H). ^{13}C NMR (126 MHz, $CDCl_3$) δ 168.5, 168.0, 161.3, 142.6, 139.8, 123.7, 122.3, 121.2, 118.9, 53.1, 53.0, 48.9, 34.5, 31.9, 29.9, 29.7, 29.3 (2C), 27.2, 22.8, 14.2. ESIMS calcd for $C_{21}H_{30}N_4O_2$ [M+H]$^+$, 371.24; Found, 3371.34.

*2-(decylamino)-N-(9-oxo-1,2,3,9-tetrahydropyrrolo[2,1-b]quinazolin-7-yl)acetamide(**12f**).* White solid, yield: 45 %. Mp: 189−190 °C. ^{1}H NMR (500 MHz, DMSO-d_6) δ 10.02 (s, 1H), 8.46 (d, J = 2.4 Hz, 1H), 7.93 (dd, J = 8.8, 2.5 Hz, 1H), 7.61 (d, J = 8.8 Hz, 1H), 4.21−3.82 (m, 3H), 3.12 (s, 2H), 3.11 (t, J = 7.9 Hz, 2H), 2.53 (t, J = 7.1 Hz, 2H), 2.23−2.18 (m, 2H), 1.38 (m, 2H), 1.29 (m, 2H), 1.28−1.26 (m, 12H), 0.78 (t, J = 6.8 Hz, 3H). ^{13}C NMR (126 MHz, $CDCl_3$) δ 169.5, 166.0, 164.3, 142.5, 138.8, 123.7, 122.6, 121.6, 118.7, 54.2, 54.0, 48.6, 34.9, 32.4, 31.7, 29.4, 29.7, 29.7, 29.7 (2C), 27.2, 22.3, 14.1. ESIMS calcd for $C_{23}H_{34}N_4O_2$ $[M+H]^+$, 399.28; Found, 399.35.

*2-(dodecylamino)-N-(9-oxo-1,2,3,9-tetrahydropyrrolo[2,1-b]quinazolin-7-yl)acetamide(**12g**).* White solid, yield: 35 %. Mp: 223−225 °C. ^{1}H NMR (500 MHz, DMSO-d_6) δ 10.23 (s, 1H), 8.17 (d, J = 2.4 Hz, 1H), 7.88 (dd, J = 8.8, 2.5 Hz, 1H), 7.42 (d, J = 8.8 Hz, 1H), 3.87 (t, J =7.3 Hz, 2H), 3.83 (s, 1H), 3.12 (s, 2H), 3.11 (t, J = 7.9 Hz, 2H), 2.53 (t, J = 7.1 Hz, 2H), 2.23−2.18 (m, 2H), 1.38 (m, 2H), 1.29 (m, 2H), 1.28 (m, 2H), 1.27−1.26 (m, 14H), 0.86 (t, J = 6.8 Hz, 3H). ^{13}C NMR (126 MHz, $CDCl_3$) δ 167.5, 165.0, 164.3, 142.6, 138.3, 123.4, 122.4, 121.8, 118.2, 53.1, 53.0, 48.7, 34.1, 31.4, 31.4, 29.7 (5C), 29.6 (2C), 27.1, 22.7, 14.4. ESIMS calcd for $C_{25}H_{38}N_4O_2$ $[M+H]^+$, 427.60; Found, 427.68.

*2-(hexadecylamino)-N-(9-oxo-1,2,3,9-tetrahydropyrrolo[2,1-b]quinazolin-7-yl)acetamide(**12h**).* White solid, yield: 49 %. Mp: 280−281 °C. ^{1}H NMR (500 MHz, DMSO-d_6) δ 10.23 (s, 1H), 8.47 (d, J = 2.4 Hz, 1H), 7.94 (dd, J = 8.8, 2.5 Hz, 1H), 7.43 (d, J = 8.8 Hz, 1H), 4.21 (s, 1H), 4.13 (t, J =7.3 Hz, 2H), 3.13 (s, 2H), 3.11 (t, J = 7.9 Hz, 2H), 2.53 (t, J = 7.1 Hz, 2H), 2.23−2.18 (m, 2H), 1.38 (m, 2H), 1.29 (m, 2H), 1.28 (m, 2H), 1.27−1.26 (m, 22H), 0.86 (t, J = 6.8 Hz, 3H). ^{13}C NMR (126 MHz, $CDCl_3$) δ 168.4, 166.0, 164.5, 142.5, 138.6, 123.5, 122.5, 121.6, 118.4, 54.2, 54.1, 48.6, 34.7, 31.7, 31.3, 29.8 (9C), 29.4 (2C), 27.1, 22.7, 14.4. ESIMS calcd for $C_{29}H_{46}N_4O_2$ $[M+H]^+$, 483.37; Found,

483.44.

*2-(allylamino)-N-(9-oxo-1,2,3,9-tetrahydropyrrolo[2,1-b]quinazolin-7-yl)acetamide(**12i**).* Yellow solid, yield: 58 %. Mp: 182−183 °C. ^{1}H NMR (500 MHz, $CDCl_3$) δ 9.47 (s, 1H), 8.35 (dd, J = 8.8, 2.5 Hz, 1H), 8.10 (d, J = 2.5 Hz, 1H), 7.66 (d, J = 8.8 Hz, 1H), 5.91 (ddt, J = 16.8, 10.2, 6.5 Hz, 2H), 5.30 (d, J = 8.8 Hz, 1H), 4.23 (t, J =7.3 Hz, 2H), 3.25 (m, 4H), 3.19 (t, J = 7.9 Hz, 2H), 2.26−2.21 (m, 3H). ^{13}C NMR (126 MHz, $CDCl_3$) δ 169.7, 160.7, 158.4, 145.6, 136.1, 134.0, 127.8, 126.4, 120.8, 119.2, 115.1, 58.1, 57.4, 46.5, 32.4, 19.6. ESIMS calcd for $C_{16}H_{18}N_4O_2$ $[M+H]^+$, 299.15; Found, 299.19.

*2-(but-3-en-1-ylamino)-N-(9-oxo-1,2,3,9-tetrahydropyrrolo[2,1-b]quinazolin-7-yl)acetamide(**12j**).* Yellow solid, yield: 57 %. Mp: 210−212 °C. ^{1}H NMR (500 MHz, DMSO-d_6) δ 10.20 (s, 1H), 8.50 (d, J = 2.4 Hz, 1H), 8.06 (dd, J = 8.8, 2.5 Hz, 1H), 7.59 (d, J = 8.8 Hz, 1H), 5.91 (ddt, J = 16.8, 10.2, 6.5 Hz, 2H), 5.30 (d, J = 8.8 Hz, 1H), 4.23 (t, J =7.3 Hz, 2H), 4.07 (dd, J = 15.1, 7.8 Hz, 2H), 3.55 (m, 2H), 3.27 (t, J =2.2 Hz, 2H), 3.08 (t, J = 7.9 Hz, 2H), 2.35−1.98 (m, 3H). ^{13}C NMR (126 MHz, DMSO-d_6) δ 168.7, 160.3, 159.5, 145.5, 136.9, 135.3, 127.6, 126.7, 120.8, 119.2, 115.2, 59.4, 56.7, 46.8, 42.7, 32.1, 19.5. ESIMS calcd for $C_{17}H_{20}N_4O_2$ $[M+H]^+$, 313.37; Found, 313.42.

*2-((3-methylbut-2-en-1-yl)amio)-N-(9-oxo-1,2,3,9-tetrahydropyrrolo[2,1-b]quinazolin-7-yl)acetamide (**12k**).* Yellow solid, yield: 61 %. Mp: 184−185 °C. ^{1}H NMR (500 MHz, DMSO-d_6) δ 10.85 (s, 1H), 8.47 (d, J = 2.4 Hz, 1H), 7.89 (dd, J = 8.8, 2.5 Hz, 1H), 7.66 (d, J = 8.8 Hz, 1H), 5.53 (t, J = 7.6 Hz, 1H), 4.18 (d, J = 7.6 Hz, 2H), 4.14 (s, 1H), 4.08 (t, J =7.3 Hz, 2H), 3.28 (t, J =2.3 Hz, 2H), 3.08 (t, J = 7.9 Hz, 2H), 2.24−2.16 (m, 2H), 1.85 (s, 3H), 1.75 (s, 3H). ^{13}C NMR (126 MHz, DMSO-d_6) δ 166.9, 163.2, 160.2, 146.1, 136.6, 135.8, 128.1, 126.5, 120.9, 118.8, 115.7, 58.1, 56.8, 46.8, 32.2, 26.6, 19.5, 18.9. ESIMS calcd for $C_{18}H_{22}N_4O_2$ $[M+H]^+$, 327.18; Found, 3327.22.

N-(9-oxo-1,2,3,9-tetrahydropyrrolo[2,1-b]quinazolin-7-yl)-2-(prop-2-yn-1-ylamino)acetamide ***(12l)***. Yellow solid, yield: 58 %. Mp: 183−184 °C. ^{1}H NMR (500 MHz, DMSO-d_6) δ 10.16 (s, 1H), 8.50 (d, J = 2.4 Hz, 1H), 7.98 (dd, J = 8.8, 2.4 Hz, 1H), 7.58 (d, J = 8.8 Hz, 1H), 4.12 (s, 1H), 4.08 (t, J =7.3 Hz, 2H), 3.55(m, 4H), 3.28 (t, J = 7.9 Hz, 2H), 2.57 (s, 1H), 2.29−2.21 (m, 2H). ^{13}C NMR (126 MHz, DMSO-d_6) δ 168.7, 160.3, 159.5, 145.5, 137.0, 131.1, 122.6, 120.8, 115.2, 79.4, 76.6, 56.7, 46.8, 42.7, 32.2, 19.5. ESIMS calcd for $C_{16}H_{16}N_4O_2$ $[M+H]^+$, 297.14; Found, 297.17.

2-(benzylamino)-N-(9-oxo-1,2,3,9-tetrahydropyrrolo[2,1-b]quinazolin-7-yl)acetamide ***(12m)***. Yellow solid, yield: 68 %. Mp: 188−189 °C. ^{1}H NMR (500 MHz, $CDCl_3$) δ 9.28 (s, 1H), 8.24 (dd, J = 8.8, 2.5 Hz, 1H), 8.06 (d, J = 2.5 Hz, 1H), 7.62 (d, J = 8.8 Hz, 1H), 7.42−7.40 (m, 3H), 7.34−7.29 (m, 2H), 4.57 (s, 1H), 4.25 (t, J =7.3 Hz, 2H), 3.79 (s, 4H), 3.33 (t, J = 7.9 Hz, 2H), 2.31−2.20 (m, 2H). ^{13}C NMR (126 MHz, $CDCl_3$) δ 169.3, 160.7, 158.4, 145.7, 136.7, 136.0, 129.1 (2C), 127.9 (2C), 126.3, 123.4, 122.6, 120.8, 115.0, 59.8, 58.0, 46.6, 32.4, 19.6. ESIMS calcd for $C_{20}H_{20}N_4O_2$ $[M+H]^+$, 349.17; Found, 349.23.

N-(9-oxo-1,2,3,9-tetrahydropyrrolo[2,1-b]quinazolin-7-yl)-2-((3-phenylpropyl)amino)acetamide ***(12n)***. White solid, yield: 59 %. Mp: 208−210 °C. ^{1}H NMR (500 MHz, DMSO-d_6) δ 10.49 (s, 1H), 8.46 (d, J = 2.2 Hz, 1H), 7.95 (dd, J = 8.8, 2.1 Hz, 1H),7.93 (d, J = 8.7 Hz, 2H), 7.83 (d, J = 8.0 Hz, 2H), 7.63 (d, J = 8.0 Hz, 1H), 7.61 (d, J = 8.8 Hz, 1H), 4.63 (s, 1H), 4.25 (t, J =7.3 Hz, 2H), 3.85 (s, 2H), 3.76 (t, J = 7.8 Hz, 2H), 3.38 (t, J = 7.8 Hz, 2H), 3.21 (t, J = 7.9 Hz, 2H), 2.76−2.63 (m, 2H), 2.52−2.43 (m, 2H). ^{13}C NMR (126 MHz, DMSO-d_6) δ 166.5, 160.3, 158.2, 146.9, 136.9, 136.3, 129.8 (2C), 127.8 (2C), 126.2, 123.2, 122.4, 118.6, 115.5, 46.8, 43.2, 35.5, 32.2, 27.2, 23.9, 19.5. ESIMS calcd for $C_{22}H_{24}N_4O_2$ $[M+H]^+$, 377.20; Found, 377.25.

2-((2-methylbenzyl)amino)-N-(9-oxo-1,2,3,9-tetrahydropyrrolo[2,1-b]quinazolin-7-yl)acetamide

(12o). Yellow solid, yield: 69 %. Mp: 223−225 °C. ^{1}H NMR (500 MHz, $CDCl_3$) δ 8.89 (s, 1H), 8.05 (dd, J = 8.8, 2.3 Hz, 1H), 7.92 (d, J = 2.1 Hz, 1H), 7.60 (d, J = 8.8 Hz, 1H), 7.37 (d, J = 7.4 Hz, 2H), 7.22 (dd, J = 13.2, 5.8 Hz, 2H), 4.60 (s, 1H), 4.24 (t, J =7.3 Hz, 2H), 3.80 (s, 2H), 3.34 (s, 2H), 3.19 (t, J = 7.9 Hz, 2H), 2.36−2.27 (m, 2H), 2.03 (s, 3H). ^{13}C NMR (126 MHz, $CDCl_3$) δ 169.4, 160.6, 158.3, 145.5, 136.9, 135.9, 135.4, 130.8, 130.3, 128.0, 127.6, 126.3, 126.2, 120.7, 114.8, 58.8, 58.5, 46.5, 32.4, 19.6, 19.3. ESIMS calcd for $C_{21}H_{22}N_4O_2$ $[M+H]^+$, 363.18; Found, 363.22.

2-((2-fluorobenzyl)amino)-N-(9-oxo-1,2,3,9-tetrahydropyrrolo[2,1-b]quinazolin-7-yl)acetamide ***(12p)***. White solid, yield: 70 %. Mp: 109−111 °C. ^{1}H NMR (500 MHz, $CDCl_3$) δ 9.55 (s, 1H), 8.22 (d, J = 2.2 Hz, 1H), 8.18 (dd, J = 8.8, 2.4 Hz, 1H), 7.64 (d, J = 8.8 Hz, 1H), 7.15 (d, J = 7.4 Hz, 2H), 7.13−7.06 (m, 2H), 4.56 (s, 1H), 4.28−4.22 (m, 2H), 3.85 (s, 2H), 3.34 (s, 2H), 3.21 (t, J = 7.9 Hz, 2H), 2.37−2.29 (m, 2H). ^{13}C NMR (126 MHz, $CDCl_3$) δ 169.1, 161.7 (d, $^{1}J_{CF}$ = 245.5 Hz), 158.3, 145.5, 136.2, 134.9, 131.7 (d, $^{3}J_{CF}$ = 4.0 Hz), 129.9 (d, $^{3}J_{CF}$ = 8.7 Hz), 127.6, 126.3, 124.4, 124.3 (d, $^{2}J_{CF}$ = 19.0 Hz), 120.8, 115.8 (d, $^{2}J_{CF}$ = 12.5 Hz), 115.2, 58.1, 53.9, 46.5, 32.4, 19.6. ESIMS calcd for $C_{20}H_{19}FN_4O_2$ $[M+H]^+$, 367.16; Found, 367.19.

2-((3,5-difluorobenzyl)amino)-N-(9-oxo-1,2,3,9-tetrahydropyrrolo[2,1-b]quinazolin-7-yl)acetamide ***(12q)***. White solid, yield: 64 %. Mp: 266−268 °C. ^{1}H NMR (500 MHz, DMSO-d_6) δ 10.02 (s, 1H), 8.46 (d, J = 2.5 Hz, 1H), 7.93 (dd, J = 8.8, 2.5 Hz, 1H), 7.58 (d, J = 8.8 Hz, 1H), 7.21 (d, J = 1.9 Hz, 2H), 7.10 (tt, J = 9.3, 2.2 Hz, 1H), 4.48 (s, 1H), 4.09 (t, J = 7.4 Hz, 2H), 3.86 (s, 2H), 3.39 (s, 2H), 3.09 (t, J = 7.9 Hz, 2H), 2.25 – 2.15 (m, 2H). ^{13}C NMR (126 MHz, DMSO-d_6) δ 169.5, 162.9 (d, $^{1}J_{CF}$ = 245.9, 2C), 160.3, 159.5, 145.6, 144.2 (t, $^{3}J_{CF}$ = 8.8 Hz), 136.9, 127.5, 126.7, 120.8, 115.4, 112.0 (dd, $^{2}J_{CF}$ = 19.6 Hz, $^{3}J_{CF}$ = 5.4 Hz, 2C), 103.0 (t, $^{2}J_{CF}$ = 25.8 Hz), 57.6, 57.1, 46.8, 32.2, 19.5. ESIMS calcd for $C_{20}H_{18}F_2N_4O_2$ $[M+H]^+$, 385.15; Found, 385.20.

2-((2-nitrobenzyl)amino)-N-(9-oxo-1,2,3,9-tetrahydropyrrolo[2,1-b]quinazolin-7-yl)acetamide ***(12r)***. White solid, yield: 73 %. Mp: 178−180 °C. ^{1}H NMR (500 MHz, DMSO-d_6) δ 10.16 (s, 1H), 8.49 (d, J = 2.2 Hz, 1H), 8.04 (d, J = 8.0 Hz, 1H), 7.95 (dd, J = 8.8, 2.1 Hz, 1H), 7.83−7.60 (m, 3H), 7.58 (d, J = 8.8 Hz, 1H), 4.61 (s, 1H), 4.08 (t, J =7.2 Hz, 2H), 3.79 (s, 2H), 3.48 (s, 2H), 3.158 (t, J = 7.8 Hz, 2H), 2.56−2.48 (m, 2H). ^{13}C NMR (126 MHz, DMSO-d_6) δ 168.5, 166.2, 161.3, 146.6, 146.2, 139.9, 128.5, 127.7, 123.8, 122.6, 121.8, 119.8, 117.4, 115.0, 112.4, 53.7, 52.1, 51.3, 36.2, 19.9. ESIMS calcd for $C_{20}H_{19}N_5O_4$ $[M+H]^+$, 394.15; Found, 394.21.

2-((2-cyanobenzyl)amino)-N-(9-oxo-1,2,3,9-tetrahydropyrrolo[2,1-b]quinazolin-7-yl)acetamide ***(12s)***. White solid, yield: 71 %. Mp: 115−117 °C. ^{1}H NMR (500 MHz, DMSO-d_6) δ 10.23 (s, 1H), 8.32 (d, J = 2.7 Hz, 1H), 8.17(d, J = 8.0 Hz, 1H), 7.95 (dd, J = 8.8, 2.1 Hz, 1H), 7.81−7.67 (m, 3H), 7.58 (d, J = 8.8 Hz, 1H), 4.32 (s, 1H), 4.16 (t, J =7.2 Hz, 2H), 3.93 (s, 2H), 3.56 (s, 2H), 3.08 (t, J = 7.8 Hz, 2H), 2.24−2.16 (m, 2H). ^{13}C NMR (126 MHz, DMSO-d_6) δ 170.3, 160.3, 159.5, 146.4, 145.5, 137.0, 132.6, 132.5, 129.5, 127.6, 127.4, 126.4, 120.8, 119.4, 115.0, 110.1, 62.7, 52.3, 46.7, 32.1, 19.5. ESIMS calcd for $C_{21}H_{19}N_5O_2$ $[M+H]^+$, 373.15; Found, 373.19.

4.3. hAChE and hBChE Inhibition Assays

AChE and BChE inhibitory activities for the tested compounds were obtained using the method of Ellman et al[47]. *h*AChE, *h*BChE, 5,5′-dithiobis(2-nitrobenzoic acid) (Ellman's reagent; DTNB), acetylthiocholine iodide (ATCI), and butyrylthiocholine iodide (BTCI) were purchased from Sigma-Aldrich. At least five different concentrations (10^{-4}–10^{-9} M) of each test compound were used to determine the enzyme inhibition activity. In summary, the procedure was as follows: 50 μL of *h*AChE (0.02 unit/mL) or *h*BChE (0.02 unit/mL) and 10 μL of the compounds was incubated at

37 °C for 6 min; next, 30 μL of 0.01 M substrate (ATCI or BTCI solution) was added, and the solution further incubated at 37 °C for 12 min; and, finally, 150 μL of 0.01 M DTNB was added, and the activity measured at a wavelength of 415 nm using an Evolution 300 PC UV-Vis Spectrophotometer. The IC_{50} value (the concentration of the compound required for a 50% reduction in cholinesterase activity) was calculated using Origin 8.0 software. The results are expressed as the mean ± SEM of at least four experiments performed in triplicate.

4.4. Kinetic Study of AChE Inhibition Assay

The mechanism of AChE inhibition by compound **12q** was determined by using Ellman's method [49]. Relatively low concentrations of the substrate (0.1−0.5 mM) were reacted with AChE in the absence or presence of different concentrations of compound **12q** (1−10 nM). The V_{max} and K_m values for Michaelis−Menten kinetics were obtained by a weighted least squares analysis from the substrate–velocity curves using GraphPad Prism 5. In addition, the inhibitor constant (K_i) was calculated by linear regression from the Lineweaver−Burk plot versus the inhibitor concentration, and the K_i' values were determined by plotting the apparent $1/v_{max}$ versus inhibitor concentration.

4.5. Aβ1−42 Self-aggregation Inhibition Assay

The thioflavin T fluorescence method was used to quantify amyloid fibril formation[46]. Thioflavin T, $A\beta_{1-42}$, and 1,1,1,3,3,3-hexafluoro-2-propanol (HFIP) were acquired from Sigma-Aldrich. HFIP-pretreated $A\beta_{1-42}$ samples were dissolved in a 50 mM phosphate buffer (pH 7.4), to obtain a stable stock solution (Aβ concentration of 500 μM). The peptide was incubated in 10 mM phosphate buffer (pH 8.0) at 30 °C for 24 h (final Aβ concentration of 50 μM) with or without

the tested compounds at 10 μM (Aβ : inhibitor = 5:1). After incubation, the samples were diluted to a final volume of 200 μL with 50 mM glycine−NaOH buffer (pH 8.5) containing 1.5 μM thioflavin T. Next, a 300 s time scan of the fluorescence intensity was carried out (λ_{exc} = 446 nm, λ_{em} = 490 nm), and the plateau values averaged after subtracting the background fluorescence of the thioflavin T solution. The percentage inhibition was calculated by the following formula:

$$\text{inhibition (\%)} = (1 - IF_i/IF_o) \times 100$$

where IF_i and IF_o are the fluorescence intensities obtained from Aβ_{1-42} in the presence and absence of inhibitor, respectively.

4.6. Metal-Chelating Assay

Compound **12q** was investigated as a metal chelator using UV−vis and fluorescence spectrophotometers in 20 % (*v*/*v*) ethanol/buffer (20 mM HEPES, 150 mM NaCl, pH 7.4). A fixed amount of compound **12q** (50 μM) was mixed with increasing amounts of Cu(II), Fe(II), Fe(III), and Zn(II) (0−1000 μM) for 30 min, and the fluorescence intensity (λ_{exc} = 285 nm) examined. In addition, the UV absorption spectra of compound **12q** (50 μM, final concentration) alone or in the presence of $CuSO_4$, $FeSO_4$, $FeCl_3$, or $ZnCl_2$ (50 μM) were recorded at room temperature. To obtain the stoichiometry of the compound–Cu^{2+} complex, a fixed amount of compound **12q** (50 μM) was mixed with increasing amounts of Cu^{2+} (0−100 μM), and the difference in the UV spectra assessed to give the ligand:metal ratio in the complex.

Acknowledgements

This work was supported by grants from the Program for Natural Science Foundation of China

(Grant No. 21602178).

Conflicts of interest

The authors declare no conflict of interest about this article.

References

[1] D.M. Walsh, D.J. Selkoe, Deciphering the Molecular Basis of Memory Failure in Alzheimer's Disease, Neuron, 44 (2004) 181-193.

[2] The Global Voice on Dementia, Alzheimer's Disease International, World Alzheimer Report. https://www.alz.co.uk/research/WorldAlzheimerReport2016.pdf (accessed April 24, 2016).

[3] M. Prince, R. Bryce, E. Albanese, A. Wimo, W. Ribeiro, C.P. Ferri, The global prevalence of dementia: A systematic review and metaanalysis, Alzheimer's & Dementia, 9 (2013) 63-75.e62.

[4] K. Blennow, M.J. de Leon, H. Zetterberg, Alzheimer's disease, The Lancet, 368 (2006) 387-403.

[5] D. Munoz-Torrero, Acetylcholinesterase Inhibitors as Disease-Modifying Therapies for Alzheimer's Disease, Current Medicinal Chemistry, 15 (2008) 2433-2455.

[6] A.B. Young, Four Decades of Neurodegenerative Disease Research: How Far We Have Come!, The Journal of Neuroscience, 29 (2009) 12722-12728.

[7] M. Goedert, M.G. Spillantini, A Century of Alzheimer's Disease, Science, 314 (2006) 777-781.

[8] D.J. Bonda, X. Wang, G. Perry, A. Nunomura, M. Tabaton, X. Zhu, M.A. Smith, Oxidative stress in Alzheimer disease: A possibility for prevention, Neuropharmacology, 59 (2010) 290-294.

[9] B. Sameem, M. Saeedi, M. Mahdavi, A. Shafiee, A review on tacrine-based scaffolds as multi-target drugs (MTDLs) for Alzheimer's disease, European Journal of Medicinal Chemistry, 128 (2016) 332.

[10] H.B. Allen, Alzheimer's Disease: Assessing the Role of Spirochetes, Biofilms, the Immune System, and Amyloid-beta with Regard to Potential Treatment and Prevention, J. Alzheimers Dis., 53 (2016) 1271-1276.

[11] E. Bossy-Wetzel, R. Schwarzenbacher, S.A. Lipton, Molecular pathways to neurodegeneration, Nature Medicine, 10 (2004) S2-S9.

[12] Z. Wang, Y. Wang, W. Li, F. Mao, Y. Sun, L. Huang, X. Li, Design, synthesis, and evaluation of multitarget-directed selenium-containing clioquinol derivatives for the treatment of Alzheimer's disease, Acs Chemical Neuroscience, 5 (2014) 952-962.

[13] F. Zemek, L. Drtinova, E. Nepovimova, V. Sepsova, J. Korabecny, J. Klimes, K. Kuca, Outcomes of Alzheimer's disease therapy with acetylcholinesterase inhibitors and memantine, Expert Opinion on Drug Safety, 13 (2014) 759-774.

[14] A. Więckowska, M. Kołaczkowski, A. Bucki, J. Godyń, M. Marcinkowska, K. Więckowski, P. Zaręba, A. Siwek, G. Kazek, M. Głuch-Lutwin, Novel multi-target-directed ligands for Alzheimer's disease: Combining cholinesterase inhibitors and 5-HT6 receptor antagonists. Design, synthesis and biological evaluation, European Journal of Medicinal Chemistry, 124 (2016) 63-81.

[15] F. Prati, S.A. De, P. Bisignano, A. Armirotti, M. Summa, D. Pizzirani, R. Scarpelli, D.I. Perez, V. Andrisano, A. Perez-Castillo, Multitarget Drug Discovery for Alzheimer's Disease: Triazinones as BACE-1 and GSK-3β Inhibitors, Angewandte Chemie International Edition, 54 (2015) 1578-1582.

[16] T.-I. Kam, Y. Gwon, Y.-K. Jung, Amyloid beta receptors responsible for neurotoxicity and cellular defects in Alzheimer's disease, Cellular and Molecular Life Sciences, 71 (2014) 4803-4813.

[17] S. Sisodia, E. Koo, K. Beyreuther, A. Unterbeck, D. Price, Evidence that beta-amyloid protein in Alzheimer's disease is not derived by normal processing, Science, 248 (1990) 492-495.

[18] T. Golde, S. Estus, L. Younkin, D. Selkoe, S. Younkin, Processing of the amyloid protein precursor to potentially amyloidogenic derivatives, Science, 255 (1992) 728-730.

[19] B. De Strooper, R. Vassar, T. Golde, The secretases: enzymes with therapeutic potential in Alzheimer disease, Nature Reviews Neurology, 6 (2010) 99-107.

[20] M. Hernandez-Rodriguez, J. Correa-Basurto, F. Martinez-Ramos, I. Irene Padilla-Martinez, C.G. Benitez-Cardoza, E. Mera-Jimenez, M. Cecilia Rosales-Hernandez, Design of Multi-Target Compounds as AChE, BACE1, and Amyloid-beta(1-42) Oligomerization Inhibitors: In Silico and In Vitro Studies, J. Alzheimers Dis., 41 (2014) 1073-1085.

[21] P. Davies, A.J. Maloney, Selective loss of central cholinergic neurons in Alzheimer's disease, Lancet, 2 (1976) 1403.

[22] R.M. Nitsch, B.E. Slack, R.J. Wurtman, J.H. Growdon, Release of Alzheimer amyloid precursor derivatives stimulated by activation of muscarinic acetylcholine receptors, Science, 258 (1992) 304-307.

[23] N.C. Inestrosa, A. Alvarez, C.A. Pérez, R.D. Moreno, M. Vicente, C. Linker, O.I. Casanueva, C. Soto, J. Garrido, Acetylcholinesterase accelerates assembly of amyloid-beta-peptides into Alzheimer's fibrils: possible role of the peripheral site of the enzyme, Neuron, 16 (1996) 881-891.

[24] A. Krasiński, Z. Radić, R. Manetsch, J. Raushel, P. Taylor, K.B. Sharpless, H.C. Kolb, In Situ Selection of Lead Compounds by Click Chemistry: Target-Guided Optimization of Acetylcholinesterase Inhibitors, Journal of the American Chemical Society, 127 (2005) 6686-6692.

[25] C. Zhang, Q.Y. Du, L.D. Chen, W.H. Wu, S.Y. Liao, L.H. Yu, X.T. Liang, Design, synthesis and evaluation of novel tacrine-multialkoxybenzene hybrids as multi-targeted compounds against Alzheimer's disease, European Journal of Medicinal Chemistry, 116 (2016) 200-209.

[26] C.G. Ballard, N.H. Greig, A.L. Guillozetbongaarts, A. Enz, S. Darvesh, Cholinesterases: roles in the brain during health and disease, Current Alzheimer Research, 2 (2005) 307-318.

[27] Y. Furukawahibi, T. Alkam, A. Nitta, A. Matsuyama, H. Mizoguchi, K. Suzuki, S. Moussaoui, Q.S. Yu, N.H. Greig, T. Nagai, Butyrylcholinesterase inhibitors ameliorate cognitive dysfunction induced by amyloid-β peptide in mice, Behavioural Brain Research, 225 (2011) 222-229.

[28] M.F. Eskander, N.G. Nagykery, E.Y. Leung, B. Khelghati, C. Geula, Rivastigmine is a potent inhibitor of acetyl- and butyrylcholinesterase in Alzheimer's plaques and tangles, Brain Research, 1060 (2005) 144-152.

[29] E. Nepovimova, J. Korabecny, R. Dolezal, K. Babkova, A. Ondrejicek, D. Jun, V. Sepsova, A. Horova, M. Hrabinova, O. Soukup, N. Bukum, P. Jost, L. Muckova, J. Kassa, D. Malinak, M. Andrs, K. Kuca, Tacrine-Trolox Hybrids: A Novel Class of Centrally Active, Nonhepatotoxic Multi-Target-Directed Ligands Exerting Anticholinesterase and Antioxidant Activities with Low In Vivo Toxicity, Journal of Medicinal Chemistry, 58 (2015) 8985-9003.

[30] A.I. Bush, Drug development based on the metals hypothesis of Alzheimer's disease, Journal of Alzheimers Disease Jad, 15 (2008) 223-240.

[31] T. Amit, Y. Avramovich-Tirosh, M.B. Youdim, S. Mandel, Targeting multiple Alzheimer's disease etiologies with multimodal neuroprotective and neurorestorative iron chelators, Faseb Journal Official Publication of the Federation of American Societies for Experimental Biology, 22 (2008) 1296-1305.

[32] X. Huang, C.S. Atwood, M.A. Hartshorn, G. Multhaup, L.E. Goldstein, R.C. Scarpa, M.P. Cuajungco, D.N. Gray, J. Lim, R.D. Moir, The Aβ Peptide of Alzheimer's Disease Directly Produces Hydrogen Peroxide through Metal Ion Reduction , Biochemistry, 38 (1999) 7609-7616.

[33] X.-j. Zhao, Y.-r. Jiang, D. Guo, D.-m. Gong, Y. Zhu, Y.-c. Deng, Multipotent AChE and BACE-1 inhibitors for the treatment of Alzheimer's disease: Design, synthesis and bio-analysis of 7-amino-1,4-dihydro-2 H -isoquilin-3-one derivates, European Journal of Medicinal Chemistry, 138 (2017) 738-747.

[34] Z. Wang, Y. Wang, W. Li, F. Mao, Y. Sun, L. Huang, X. Li, Design, Synthesis, and Evaluation of Multitarget-Directed Selenium-Containing Clioquinol Derivatives for the Treatment of Alzheimer's Disease, Acs Chemical Neuroscience, 5 (2014) 952-962.

[35] G. Sharma, S. Laxman, Y. Murthy, K.A. Lakshmi, Ramji, M. Tark, Synthesis of Novel Deoxyvasicinone Analogs and their Anti-Bacterial Studies, IJAPBC, 1 (2014) 328-333.

[36] K.M. Shakhidoyatov, B.Z. Elmuradov, Tricyclic Quinazoline Alkaloids: Isolation, Synthesis, Chemical Modification, and Biological Activity, Chemistry of Natural Compounds, 50 (2014) 781-800.

[37] H.-J. Zhong, K.-H. Leung, S. Lin, D.S.-H. Chan, Q.-B. Han, S.L.-F. Chan, D.-L. Ma, C.-H. Leung, Discovery of deoxyvasicinone derivatives as inhibitors of NEDD8-activating enzyme, Methods, 71 (2015) 71-76.

[38] F.H. Darras, S. Wehle, G. Huang, C.A. Sotriffer, M. Decker, Amine substitution of quinazolinones leads to selective nanomolar AChE inhibitors with 'inverted' binding mode, Bioorganic & Medicinal Chemistry, 22 (2014) 4867-4881.

[39] M. Decker, F. Krauth, J. Lehmann, Novel tricyclic quinazolinimines and related tetracyclic nitrogen bridgehead compounds as cholinesterase inhibitors with selectivity towards butyrylcholinesterase, Bioorganic & Medicinal Chemistry, 14 (2006) 1966-1977.

[40] F.H. Darras, S. Pockes, G. Huang, S. Wehle, A. Strasser, H.J. Wittmann, M. Nimczick, C.A. Sotriffer, M. Decker, Synthesis, biological evaluation, and computational studies of Tri- and tetracyclic nitrogen-bridgehead compounds as potent dual-acting AChE inhibitors and hH3 receptor antagonists, Acs Chemical Neuroscience, 5 (2014) 225-242.

[41] F. Darras, B. Kling, J. Heilmann, M. Decker, Neuroprotective Tri- andTetracyclic BChE InhibitorsReleasing Reversible Inhibitors upon Carbamate Transfer, Acs Medicinal Chemistry Letters, 3 (2012) 914-919.

[42] C.G. Carolan, G.P. Dillon, D. Khan, S.A. Ryder, J.M. Gaynor, S. Reidy, J.F. Marquez, M. Jones, V. Holland, J.F. Gilmer, Isosorbide-2-benzyl carbamate-5-salicylate, a peripheral anionic site binding subnanomolar selective butyrylcholinesterase inhibitor, Journal of Medicinal Chemistry, 53 (2010) 1190-1199.

[43] E. Nepovimova, E. Uliassi, J. Korabecny, L.E. Peñaaltamira, S. Samez, A. Pesaresi, G.E. Garcia, M. Bartolini, V. Andrisano, C. Bergamini, Multitarget drug design strategy: quinone-tacrine hybrids designed to block amyloid-β

aggregation and to exert anticholinesterase and antioxidant effects, Journal of Medicinal Chemistry, 57 (2014) 8576-8589.

[44] R. Mayeux, M.X. Tang, D.M. Jacobs, J. Manly, K. Bell, C. Merchant, S.A. Small, Y. Stern, H.M. Wisniewski, P.D. Mehta, Plasma amyloid β-peptide 1–42 and incipient Alzheimer's disease, Annals of Neurology, 46 (1999) 412-416.

[45] M. Shidore, J. Machhi, K. Shingala, P. Murumkar, M.K. Sharma, N. Agrawal, A. Tripathi, Z. Parikh, P. Pillai, M.R. Yadav, Benzylpiperidine-linked diarylthiazoles as potential anti-Alzheimer's agents-synthesis and biological evaluation, Journal of Medicinal Chemistry, 59 (2016) 5823-5846.

[46] G.V.D. Ferrari, M.A. Canales, I. Shin, L.M. Weiner, I.Silman, And, N.C.Inestrosa, A Structural Motif of Acetylcholinesterase That Promotes Amyloid β-Peptide Fibril Formation, Biochemistry, 40 (2001) 10447-10457.

[47] S. Lee, X. Zheng, J. Krishnamoorthy, M.G. Savelieff, H.M. Park, J.R. Brender, H.K. Jin, J.S. Derrick, A. Kochi, H.J. Lee, Rational Design of a Structural Framework with Potential Use to Develop Chemical Reagents That Target and Modulate Multiple Facets of Alzheimer’s Disease, Journal of the American Chemical Society, 136 (2014) 299-310.

[48] P.T. Chang, R.S. Talekar, F.L. Kung, T.R. Chern, C.W. Huang, Q.Q. Ye, M.Y. Yang, C.W. Yu, S.Y. Lai, R.R. Deore, A newly designed molecule J2326 for Alzheimer's disease disaggregates amyloid fibrils and induces neurite outgrowth, Neuropharmacology, 92 (2015) 146-157.

[49] G.L. Ellman, K.D. Courtney, A.V. Jr, R.M. Featherstone, A new and rapid colorimetric determination of acetylcholinesterase activity, Biochemical Pharmacology, 7 (1961) 88-95.

Legend of Scheme and Figures

Scheme 1. Synthesis of Deoxyvasicinone Derivatives.

Figure 1. Structures of AChE inhibitors **1**−**4** used for the management of AD.

Figure 2. Deoxyvasicinone and its derivatives.

Figure 3. Design strategy for deoxyvasicinone derivatives.

Figure 4. Kinetic study on the mechanism of *h*AChE inhibition by compound **12q**. Overlaid Lineweaver−Burk reciprocal plots of AChE initial velocity at increasing substrate concentration (0.1−0.5 mM) in the absence and in the presence (1.0−10.0 nM) of compound **12q** are shown. Lines were derived from a weighted least-squares analysis of the data points.

Figure 5. (A) Fluorescence (λ_{exc} = 285 nm) and (B) UV spectra of compound **12q** (50 μM) alone and in the presence of $CuSO_4$, $FeSO_4$, $FeCl_3$ or $ZnCl_2$ (50 μM) in 20 % (*v*/*v*) ethanol/buffer (20 mM HEPES, 150 mM NaCl, pH 7.4). (C) Determination of the stoichiometry of complex **12q**−Cu(II) by molar ratio method.

Table 1. *h*AChE and *h*BChE Inhibitory Activities (IC_{50}), Selectivity Ratios, and Inhibition of A$\beta_{1\text{-}42}$ Self-Aggregation of Compounds **1**, **5**, and **12a−12s**.

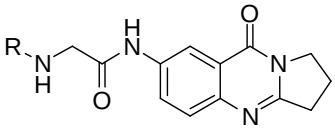

Comp.	R	*h*AChE IC_{50} (nM) ± SEM[a]	*h*BChE IC_{50} (nM) ± SEM[a]	selectivity ratio[b]	inhibition of Aβ_{1-42} self-aggregation (% ± SEM)[c]
12a	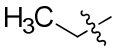	557 ± 31	1001 ± 66	0.556	6.46 ± 0.25
12b	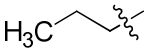	310 ± 27	1186 ± 70	0.261	7.38 ± 0.53
12c	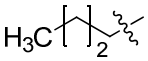	21.2 ± 1.9	107 ± 12	0.198	10.5 ± 0.82
12d	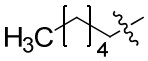	25.3 ± 1.3	10.5 ± 0.6	2.41	22.9 ± 1.3
12e	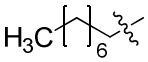	10.6 ± 0.4	45.7 ± 3.8	0.232	17.6 ± 0.9
12f	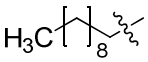	24.1 ± 2.1	37.2 ± 2.5	0.648	22.1 ± 1.5
12g	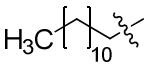	36.7 ± 1.9	26.8 ± 2.0	1.37	26.0 ± 1.7
12h	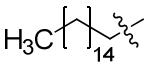	5.31 ± 2.8	4.35 ± 0.32	1.22	39.6 ± 2.2
12i	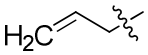	66.6 ± 5.5	16.6 ± 0.8	4.01	37.9 ± 2.5
12j	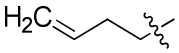	13.3 ± 0.8	81.5 ± 5.9	0.163	42.2 ± 3.1
12k	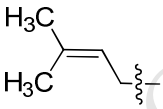	25.9 ± 1.5	16.3 ± 1.3	1.59	31.0 ± 2.4
12l	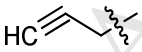	46.4 ± 2.6	12.4 ± 0.8	3.74	52.3 ± 3.8
12m	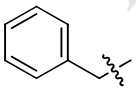	231 ± 19	145 ± 12	1.59	30.5 ± 2.5
12n	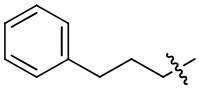	4.09 ± 0.23	20.7 ± 1.5	0.20	43.3 ± 5.1

12o	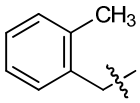	119 ± 17	107 ± 14	1.11	25.0 ± 1.6
12p	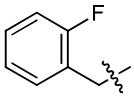	528 ± 46	108 ± 12	4.89	43.5 ± 3.2
12q	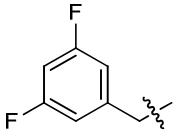	7.61 ± 0.53	2.35 ± 0.14	3.24	63.9 ± 4.9
12r	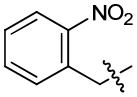	30.7 ± 2.6	103 ± 11	0.298	29.9 ± 2.4
12s	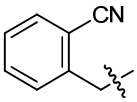	16.8 ± 0.8	29.9 ± 1.7	0.562	40.2 ± 4.2
Tacrine (**1**)		76.5 ± 3.1	10.8 ± 1.4	7.08	4.03 ± 0.55
Deoxyvasicinone (**5**)		62.5 ± 5.8 μM	45.1 ± 3.7 μM	1.39	2.53 ± 0.27
Curcumin		n.t.[d]	n.t.[d]	-	51.9 ± 2.36

[a] *h*AChE and *h*BChE: Results are the means ± SEM of at least three determinations. [b]Selectivity ratio = (IC_{50} of *h*AChE)/(IC_{50} of *h*BChE). [c]Inhibition of Aβ_{1-42} self-aggregation investigated by the thioflavin-T fluorescence assay. Assays were carried out in the presence of 10 μM inhibitor and 50 μM Aβ_{1-42}. [d]n.t. means not tested.

Scheme 1. Synthesis of Deoxyvasicinone Derivatives.[a]

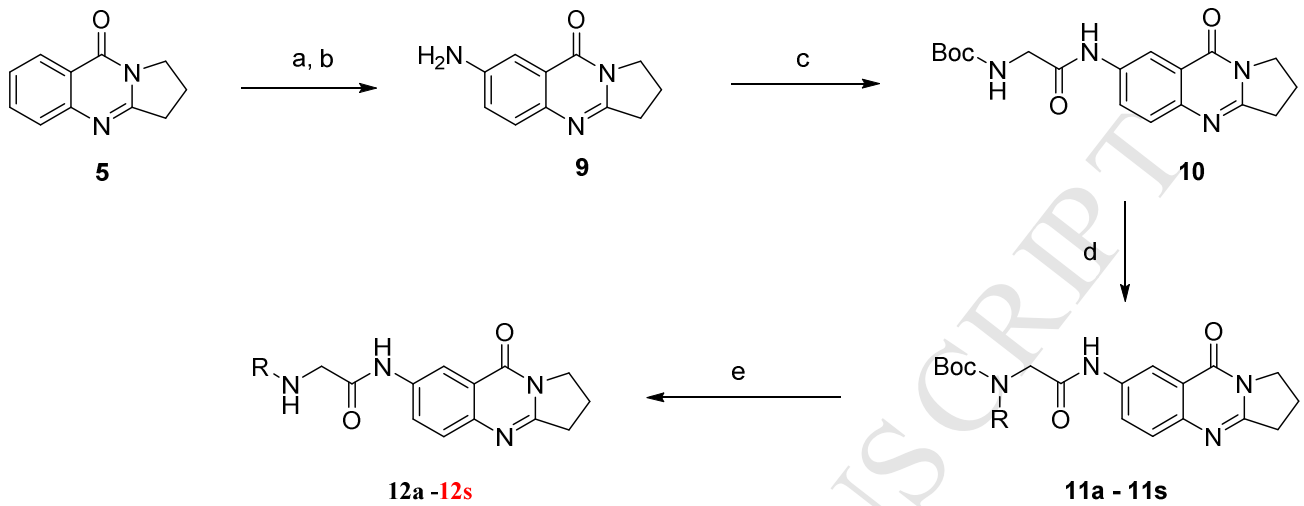

a: R = ethyl
b: R = propyl
c: R = butyl
d: R = hexyl
e: R = octyl
f: R = decyl
g: R = dodecyl
h: R = hexadecyl
i: R = allyl
j: R = but-3-en-1-yl
k: R = 3-methylbut-2-en-1-yl
l: R = prop-2-yn-1-yl
m: R = benzyl
n: R = phenylpropyl
o: R = 2-methylbenzyl
p: R = 2-fluorobenzyl
q: R = 3,5-difluorobenzyl
r: R = 2-nitrobenzyl
s: R = 3-phenylpropyl

[a]Reagents and conditions: (b) HNO_3, H_2SO_4, rt.; (b) $Na_2S{\cdot}9H_2O$, NaOH, EtOH, reflux; (c) Boc-aminoacetic acid, EDCI, dry CH_2Cl_2, reflux; (d) RBr, KI, NaH, CH_3CN, reflux; (e) CF_3COOH, dry CH_2Cl_2, reflux.

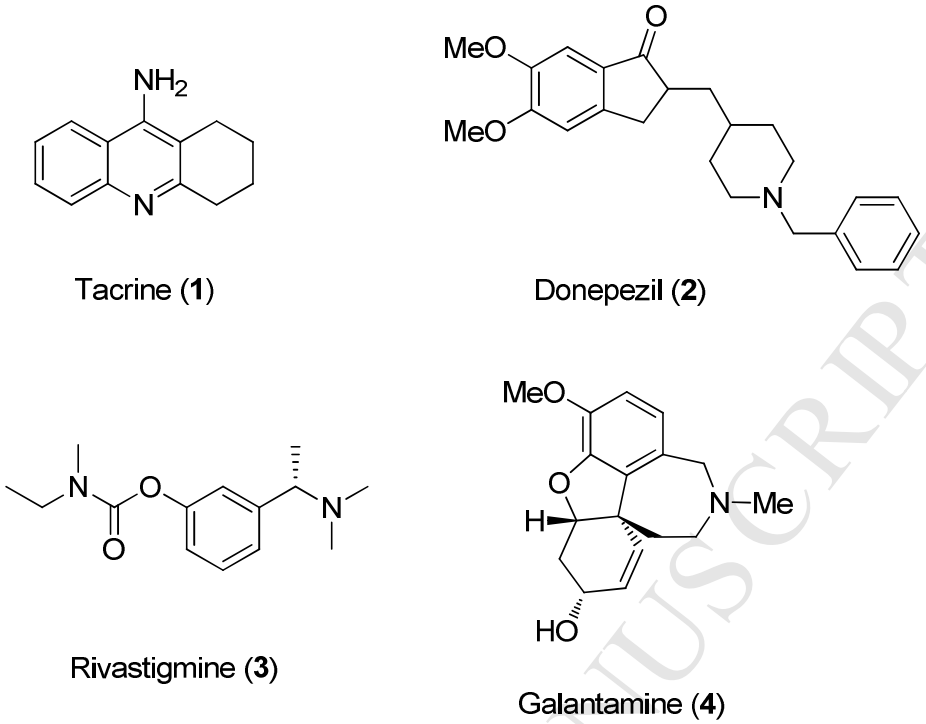

Figure 1. Structures of AChE inhibitors **1**−**4** used for the management of AD.

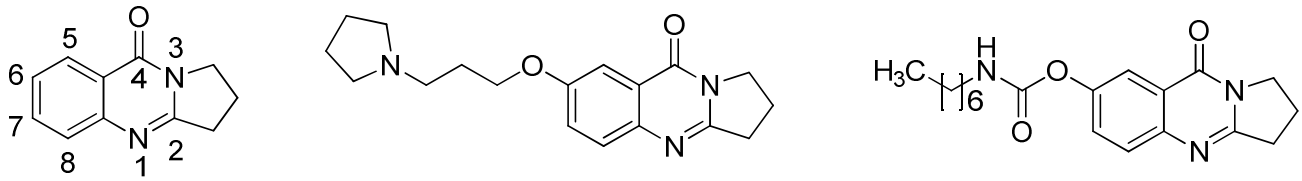

Deoxyvasicinone (**5**) **6** IC_{50} (AChE): 69.2 nM **7** IC_{50} (BChE): 1.95 μ M

Figure 2. Deoxyvasicinone and its derivatives.

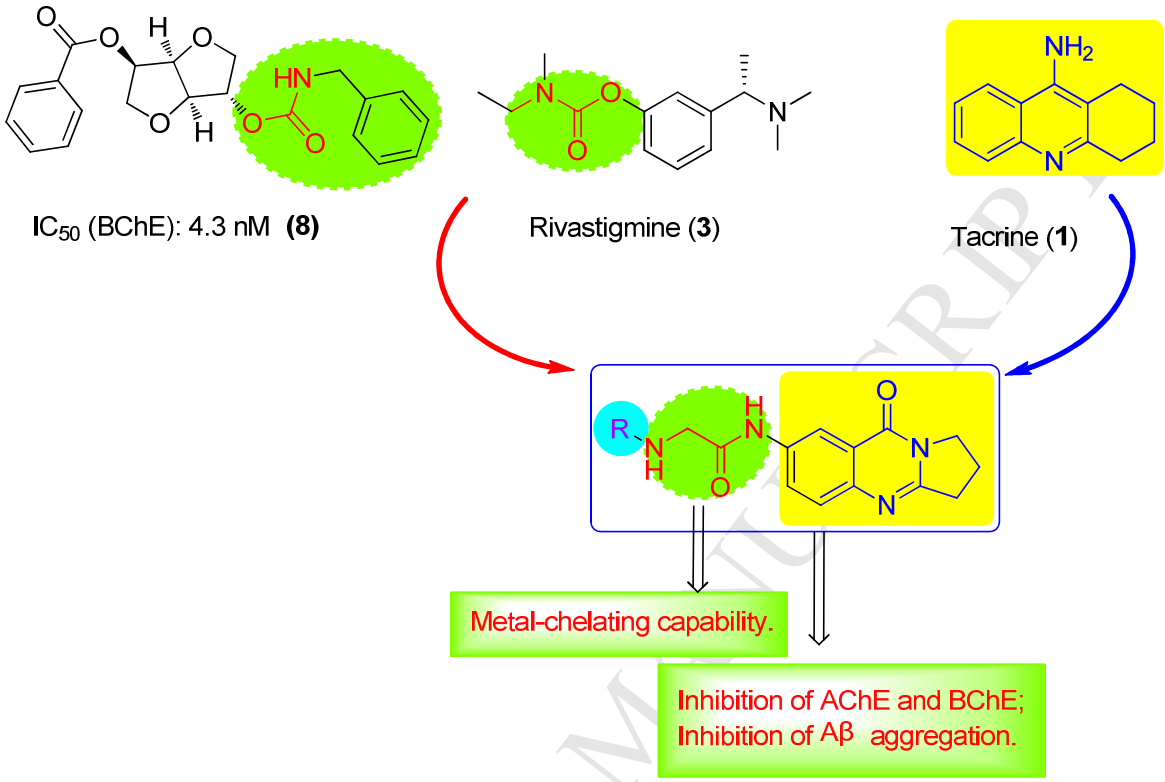

Figure 3. Design strategy for deoxyvasicinone derivatives.

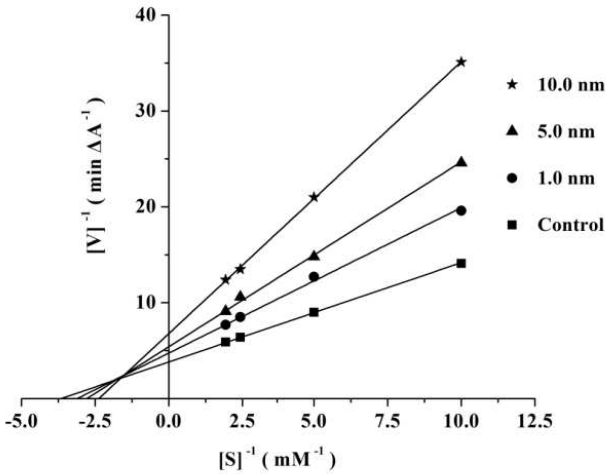

Figure 4. Kinetic study on the mechanism of *h*AChE inhibition by compound **12q**. Overlaid Lineweaver−Burk reciprocal plots of AChE initial velocity at increasing substrate concentration (0.1−0.5 mM) in the absence and in the presence (1.0−10.0 nM) of compound **12q** are shown. Lines were derived from a weighted least-squares analysis of the data points.

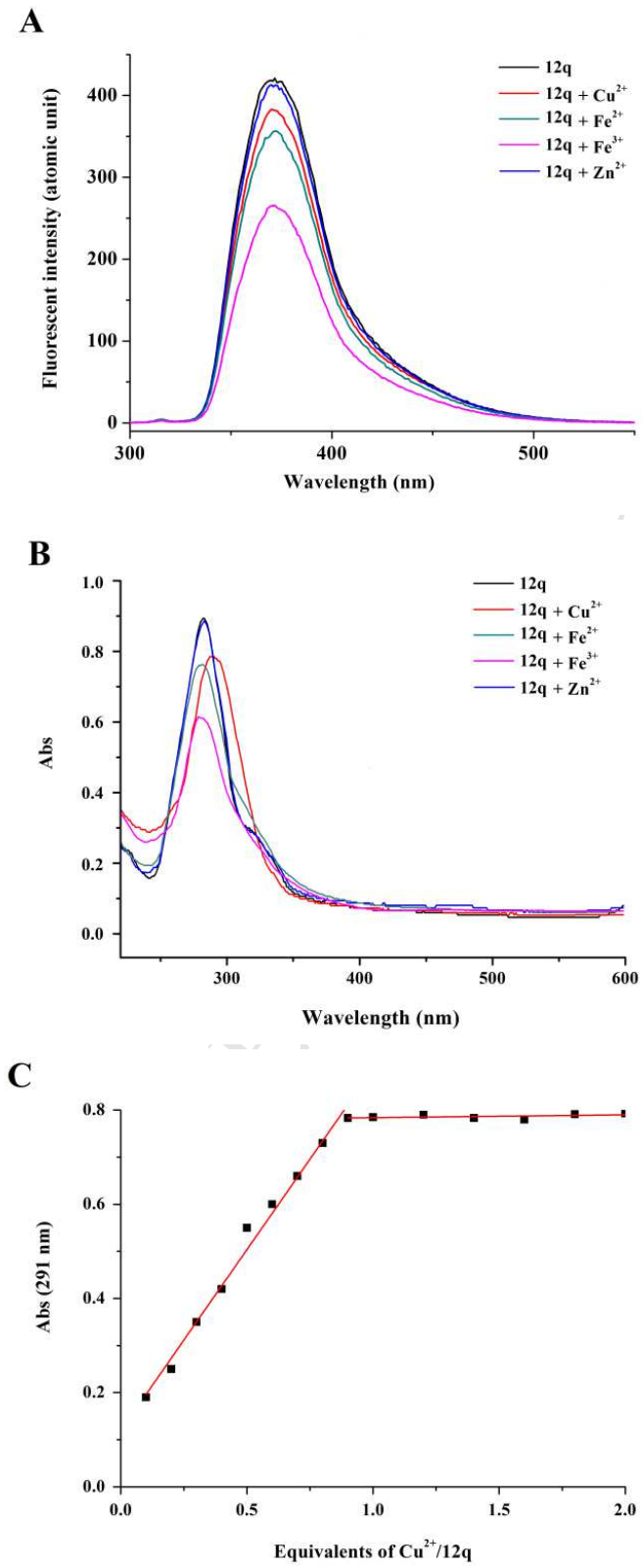

Figure 5. (A) Fluorescence (λ_{exc} = 285 nm) and (B) UV spectra of compound **12q** (50 μM) alone and in the presence of $CuSO_4$, $FeSO_4$, $FeCl_3$ or $ZnCl_2$ (50 μM) in 20 % (*v*/*v*) ethanol/buffer (20 mM HEPES, 150 mM NaCl, pH 7.4). (C) Determination of the stoichiometry of complex **12q**−Cu(II) by molar ratio method.

Highlights

- A series of novel deoxyvasicinone derivatives was synthesized.
- All derivatives showed excellent AChE and BChE inhibition activity.
- **12q** had strong inhibition on AChE and BChE with IC_{50} of 7.6 and 2.5 nM respectively.
- **12q** had the greatest ability to inhibit Aβ_{1-42} self-aggregation.
- **12q** was also an excellent metal chelator.